ADVANCED ENERGY MATERIALS
www.advenergymat.de

Electronic Conductivity of Lithium Solid Electrolytes

*Bowen Shao, Yonglin Huang, and Fudong Han**

While significant efforts are being devoted to improving the ionic conductivity of lithium solid electrolytes (SEs), electronic transport, which has an important role in the calendar life, energy density, and cycling stability of solid-state batteries (SSBs), is rarely studied. Here, the electronic conductivities of three representative SEs, including Li_3PS_4, $Li_7La_3Zr_2O_{12}$, and Li_3YCl_6, are reported. It is reported that the electronic conductivities of SEs are overestimated from the conventional measurements. By revisiting direct current polarizations using two-blocking-electrode cells and the Hebb-Wagner approach, their sources of inaccuracy are provided and the anodic decomposition of SE is highlighted as the key source for the overestimated result. Modifications in the electrode selection and data interpretation are also proposed to approach the intrinsic electronic conductivity of SEs. A two-step polarization method is also proposed to estimate the electronic conductivity of sulfides that decompose during measurement. Measured by the modified approach, the electronic conductivities of all SEs are one or two orders of magnitude lower than the reported value. Despite that, the electronic conductivity of sulfides seems to be still quite high to enable SSBs with a long calendar life of >10 years, highlighting the critical need for a more careful study of electronic transport in lithium SEs.

1. Introduction

The development of next-generation batteries has largely transitioned to a concept of "solid-state battery (SSB)" because of its great potential in improving the safety and energy density of today's lithium-ion batteries.[1–5] As the key components of an SSB, solid electrolytes (SEs) have attracted intense research interest in the past decades.[6–11] An ideal SE should have a high ionic conductivity but a low electronic conductivity so that only Li ions are mobile between electrodes. Ionic conductivity has been considered the major criterion for SE development. The discovery and development of several superionic conductors including sulfides (Li_2S-P_2S_5 and its derivatives),[6–9] oxides (e.g., Li-garnets),[10] and halides (Li-M-X, where M is a metal and X is a halide element),[11,12] with an ionic conductivity of 10^{-4} to10^{-2} S cm^{-1} which is close to or even higher than that of the liquid electrolytes, have been stimulating the research on SSBs. The electronic conductivity of SEs, on the other hand, has not been well studied. A major reason is that the reported electronic conductivity of most SEs is far lower than the ionic one and it has been taken for granted that such slight electronic conduction is negligible. **Figure 1** summarizes the electronic conductivity of typical SEs reported in the literature. The electronic conductivities of SEs are typically measured by the direct current (DC) polarization of an ion-blocking cell with either two blocking electrodes (BEs) such as Au/SE/Au or one reversible electrode (RE) and one BE such as Li/SE/Au (Figure 1B). The conductivity measurement on a cell with one RE and one BE is also called Hebb–Wagner approach.[13,14] Under DC polarization, initially all the charge carriers migrate, but since there are no ion sources provided by the blocking electrode, at the steady state the measured current is considered solely from electronic carriers, and the electronic conductivity can then be determined from this current (see Figure S1, Supporting Information, and theoretical considerations of Hebb–Wagner approach in the Supporting Information).[15–18] Measured by these approaches, the electronic conductivities of sulfides, halides, and (Li-garnet) oxides are within the range of 10^{-9} to 10^{-7} S cm^{-1} (Figure 1C and Table S1, Supporting Information) which are several orders of magnitude lower than the ionic ones. It is then believed that such slight electronic conduction in SEs will not cause detrimental effects on battery performances.

However, large discrepancies exist between the reported electronic conductivity and existing results. One direct consequence of electronic conduction in SEs would be the self-discharge of SSBs caused by electronic leakage. For a typical lab-scale 4 V SSB with a 1 mAh cm^{-2} areal capacity and 1 mm thick SE, assuming electronic conduction in SE follows Ohm's law, a 10^{-8} S cm^{-1} electronic conductivity will lead to a 20% decrease in the cell capacity after 21 days' storage (i.e., a calendar life of 21 days) (see detailed calculations in the Supporting Information). Such a fast capacity decay during aging has not been observed experimentally, even at elevated temperatures when the electronic conductivity increases, although the exact calendar life of SSBs has not been carefully studied. In addition, the reported electronic conductivity is also inconsistent with the

B. Shao, Y. Huang, F. Han
Department of Mechanical
Aerospace, and Nuclear Engineering
Rensselaer Polytechnic Institute
Troy, NY 12180, USA
E-mail: hanf2@rpi.edu

The ORCID identification number(s) for the author(s) of this article can be found under https://doi.org/10.1002/aenm.202204098.

DOI: 10.1002/aenm.202204098

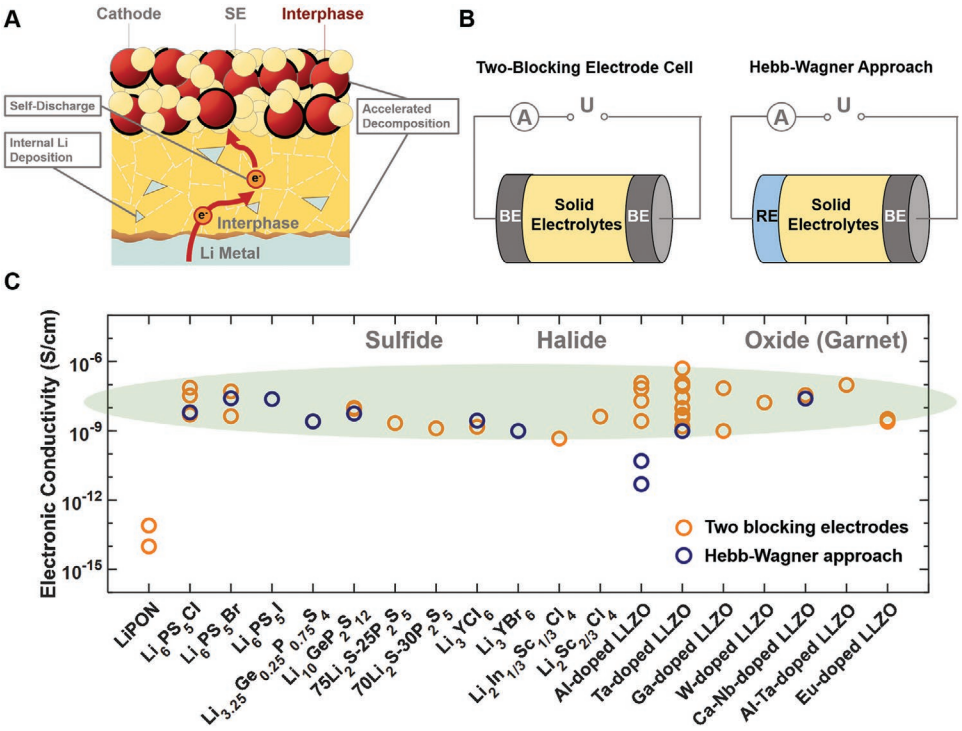

Figure 1. A) Electronic conductivity in SEs can lead to cell self-discharge, internal deposition of Li dendrites, and accelerated decompositions of SEs at the electrode/electrolyte interfaces. B) Ion blocking cells with two blocking electrodes or one reversible and one blocking electrode for measuring the electronic conductivity of SEs. C) A summary of the reported electronic conductivities of sulfide, halide, and oxide (garnet) SEs. Detailed information of the electronic conductivity data is included in Table S1, Supporting Information.

large bandgaps (3.7 eV for β-Li_3PS_4,[19] 4.6 eV for Li_3YCl_6,[20] and 6.4 eV for LLZO[21] computed from density functional theory. For materials with such a wide bandgap, the thermal energy at room temperature is usually considered insufficient to form free electronic carriers by directly exciting electrons from the valence band to the conduction band, and therefore none of the SEs should have electronic conductivity close to 10^{-8} S cm^{-1}.[22] These discrepancies suggest that the measured values from the conventional approaches may not reflect the intrinsic electronic transport properties of those SEs. It should also be noted that recent theoretical work shows that the bandgaps may not be a good descriptor for the electronic conductivity of SEs where the point defects (both intrinsic and extrinsic) can play an important role in the electronic transport properties.[23–25]

While the above-mentioned discrepancies imply that the intrinsic electronic conductivities of SEs should be lower than the reported values, they are never zero, and therefore any SE can essentially be considered as a mixed ionic and electronic conductor. It should be noted that even very small electronic conductivity can lead to perceptible self-discharge especially when the battery is not under constant use (Figure 1A).[26] While SSBs based on LiPON thin-film electrolyte have been demonstrated to have a calendar life of >10 years,[27] we propose that long calendar life cannot be assumed for bulk-type SSBs based on sulfide, Li-garnet oxide, and halide SEs due to the drastically different electronic conductivity of SEs (the electronic conductivity of LiPON is 10^{-14} to 10^{-13} S cm^{-1}).[27–30] Whether the electronic conductivity of the bulk-type SEs is sufficiently low to enable a long calendar life remains unknown for the SSB community. If we do a similar rough estimate for a future 4 V SSB with a 5 mAh cm^{-2} areal capacity and a 30-µm-thick SE using Ohm's law, the electronic conductivity of the SE should be lower than 5.7×10^{-12} S cm^{-1} to enable a long calendar life of 15 years. In addition to electronic leakage, recent works also indicate that the inherent electronic conductivity in SEs, despite being very small, can cause internal deposition of lithium dendrites inside the bulk SEs when Li metal was used as the anode, leading to cell shorting.[31,32] As the energy density of SSBs can hardly be comparable with that of conventional lithium-ion batteries unless Li is used as the anode,[1,3] understanding the electronic transport and conduction mechanisms in battery SEs is critical to develop high-energy-density SSBs. Moreover, recent reports by Nazar and Janek [33,34] proposed that the intrinsic electronic conductivity of halide-based SEs also plays a key role in the electrochemical stability of SEs in SSBs, that is, SEs with a lower electronic conductivity tend to have less decomposition when used with high voltage cathodes, and therefore understanding the intrinsic properties of electronic conduction in SEs also has important implications in improving the interfacial stability and cycling stability of high-voltage SSBs.

It should also be noted that most previous research on the electronic conductivity of SEs reported a single value as the electronic conductivity of a particular SE. However, because the concentrations of electronic carriers in a SE change with Li activity, the electronic conductivity of Li SEs depends on the Li

activity which changes in the bulk electrolyte when the cell was polarized (see Supporting Information).[26,35,36] The dependence of electronic conductivity on Li chemical potential has been studied in several theoretical works.[23–25] It has also been reported that the electronic conductivity of oxygen ion conductors can change >3 orders of magnitude as the O_2 partial pressure changes from 10^5 to 10^{-16} Pa.[37] Since the lithium activity changes by tens of orders of magnitude in the case of a 4 V SSB, one would expect a drastic change in the electronic conductivity at different locations of the SE in a real battery. This also means that the measured electronic conductivity from a cell where the Li activity of the SE is either unknown (e.g., in the cell with two blocking electrodes) or different from that in an SSB cannot reflect the real electronic transport property of the SE in the SSB. The Li activity or voltage dependence of electronic conductivity of SEs is essential to fully understand the effects of electronic conduction on battery performances and provides critical insights to understand the conduction mechanism, but such information has unfortunately not been revealed thus far.

While the electronic conductivities of SEs under a wide range of potentials from 0 to 4.5 V versus Li/Li^+ are important to understand the behavior of the SE in a real SSB with Li metal anode and high-voltage cathodes, determining such important information is unfortunately not always possible due to the limited electrochemical stability of SEs.[38,39] The thermodynamic electrochemical stability window of sulfide-based SEs is ≈0.4 V (from 1.7 to 2.1 V vs Li/Li^+) and most solid electrolytes are not thermodynamically stable at 0 V versus Li/Li^+.[39,40] When a SE is polarized/used at a voltage beyond its stability window, it will decompose. The electrolytic decomposition of SEs not only causes the formation of interphases that have different electronic conductivity and can alter the potential applied on the SE,[41] but also leads to ionic currents that can hardly be separated from the electronic one during electronic conductivity measurement. While it has been well-recognized that SEs can be used beyond their stability window to make a high-voltage SSB due to kinetic stabilizations, measuring and understanding the electronic conductivity of SEs that decompose remains challenging.

In this work, we report that the electronic conductivities of SEs were overestimated from the conventional measurements and present the sources for the inaccuracy for both two-blocking-electrode measurement and Hebb–Wagner approach. Based on the findings, we propose modifications in the electrode selection, measurement, and data interpretation to approach the intrinsic electronic conductivity of SEs. Three representative SEs, including Li_3PS_4 (LPS), $Li_7La_3Zr_2O_{12}$ (LLZO), and Li_3YCl_6 (LYC) were used in this work to investigate the electronic conductivity of sulfide-, oxide-, and halide-based SEs, respectively. The electronic conductivities of all three SEs are measured to be at least one or two orders lower than the reported values at typical battery operating voltages. While the lower electronic conductivity is certainly desirable for practical application, the electronic conductivity of cold-pressed sulfide SEs does not seem to be lower enough to enable SSBs with a long calendar life of >10 years, highlighting the critical need for a more detailed study of electronic conduction in SEs.

2. Results and Discussion

2.1. Electronic Conductivity Measurement Using a Two-Blocking-Electrode Cell

We first revisit the electronic conductivity measurement using two ion-blocking electrodes. 100-nm-thick Au film was sputtered on both sides of LLZO, LYC, and LPS SEs as the ion-blocking electrode. The Au/SE/Au cells were then polarized at DC voltages from 0.1 to 3 V. The current evolution under DC polarization was recorded for a duration of 3 h to determine the steady-state current (SSC). Three hours was used as the duration for polarization measurement because for most measurements the current after 3 h does not change 10% over a long period. **Figure 2**A shows typical current profiles under a polarization voltage of 0.3 V. The SSCs under different polarization voltages are included in Figure 2B. The electronic conductivities of the SE under different polarization voltages were then determined by Ohm's law, $\sigma = \frac{L}{S} \times \frac{I}{E}$, where σ is electronic conductivity, L is the thickness of the SE, S is the area of the SE, E is the polarization voltage, and I is the SSC. As shown in Figure 2C, for all SEs, an increase in the electronic conductivity can be observed as the polarization voltage increases to >0.5 V. Comparing the electronic conductivity for different SEs, a general trend of LPS > LYC > LLZO can be observed. The magnitudes of electronic conductivities of LLZO, LYC, and LPS are within the orders of 10^{-9} to 10^{-8} S cm^{-1}, consistent with the previously reported results (Figure 1C).

While the general trend for the electronic conductivity of different SEs agrees with the computed bandgaps of these materials,[19,42,43] this approach overestimates the electronic conductivity of SEs based on the following reasons. As mentioned above, the electronic conductivity of any Li SE largely depends on Li activity. However, for the cell with two Au electrodes, under a particular DC polarization only the difference between the cathode potential and anode potential is controlled and the absolute potential for each electrode is not defined. Therefore, the Li activity of each electrode is undefined. It is thus unclear which Li activity range the electronic conductivity is being measured. One can expect that the measured SSC is the maximum current that can be allowed to flow under the given polarization voltage, and therefore it has been considered that the electronic conductivity measured by a two-blocking-electrode cell can be considered as the upper limit of the electronic conductivity.[44,45] The second source that can lead to an overestimated result is the electrolytic decomposition of SEs due to the limited electrochemical stability window of SEs, particularly for sulfides. Many previous works on the electronic conductivity measurement of sulfide-based SEs used a polarization voltage of 1 V,[46,47] however, due to the limited electrochemical stability window of sulfide SEs (≈0.4 V),[38,39] during the measurement the SE will be decomposed, that is, the SE will be oxidized on one side, forming Li poor decomposition products such as S and P_2S_5, and reduced on the other side, forming Li rich compounds such as Li_2S and Li_3P with ionic current passing through the SE. The passing of ionic current within the SE during the measurement leads to an overestimated SSC as

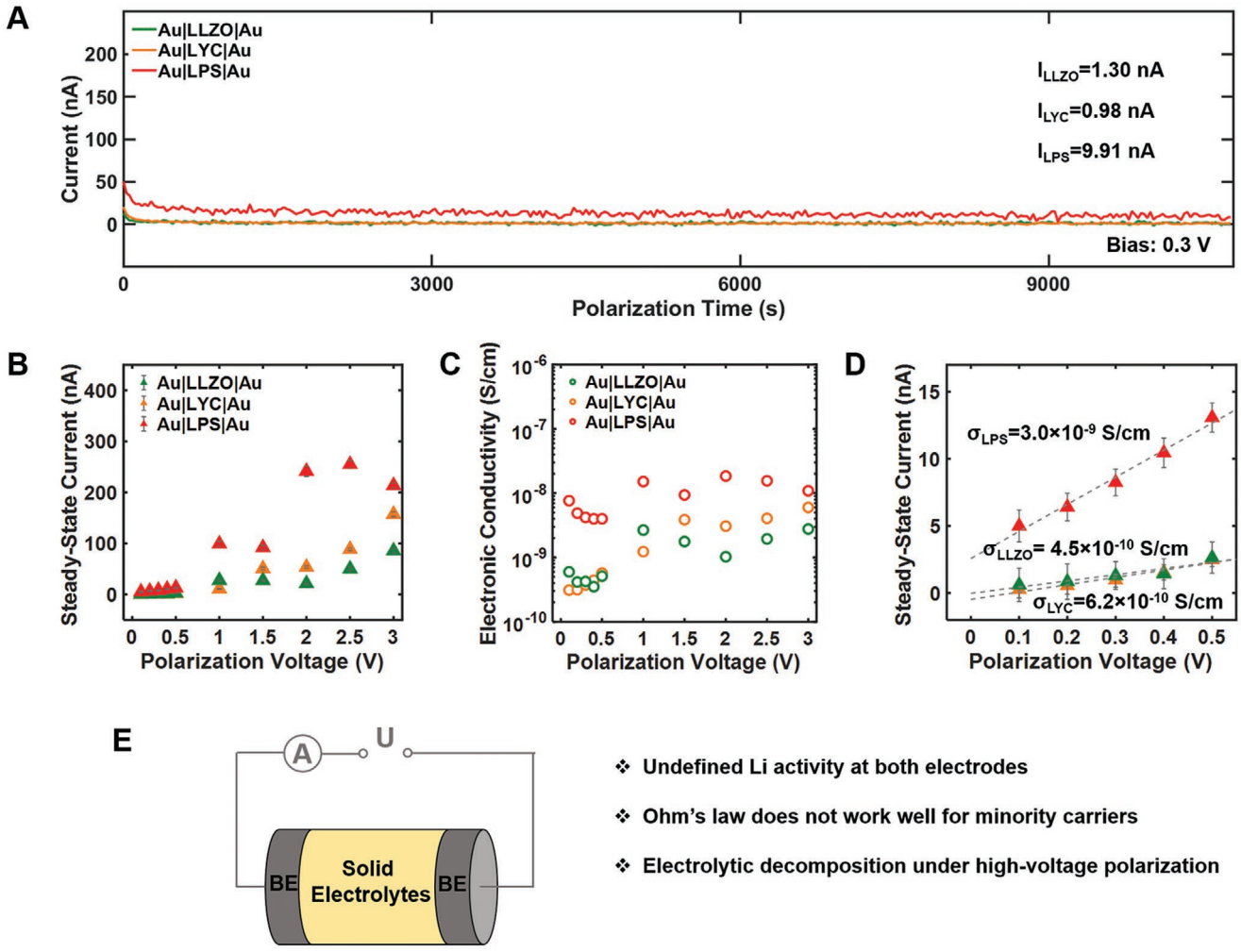

Figure 2. Electronic conductivity measurement of LLZO, LYC, and LPS SEs using a two-blocking-electrode cell. A) Current evolution of Au/LLZO/Au, Au/LYC/Au, and Au/LPS/Au cells under DC polarization of 0.3 V. The steady state current was determined at the end of the 3 h test. B) Steady-state currents of Au/LLZO/Au, Au/LYC/Au, and Au/LPS/Au cells under DC polarization at voltages from 0.1 to 3 V. C) Electronic conductivities of LLZO, LYC, and LPS at different polarization voltages. The values are determined from the steady-state currents based on Ohm's law. D) Linear fitting of the steady-state currents at low polarization voltages <0.5 V and the resultant electronic conductivity. E) Sources of inaccuracy for electronic conductivity measurement using a two-blocking-electrode cell.

the DC polarization methods assume only electronic carriers are flowing at steady state. Given that the SSC for electronic conductivity measurement is usually very small (at the order of nA or lower), even slight decomposition of SEs can lead to a significant influence on the measurement. We believe electrolytic decomposition SE is also the reason why the SSC of LPS first increases and then decreases with polarization voltages (Figure 2B). As the polarization voltage increases, the decomposition of LPS is initiated and accelerated. After the formation of a passivation layer, the decomposition reaction rate will decrease. Another source of inaccuracy for the two-blocking-electrode cell measurement arises from data analysis. Ohm's law has been used to determine the electronic conductivity of SEs measured by the two-blocking-electrode cell.[33,46,48,49] However, for superionic conductors where the concentration of ionic carriers (Li vacancies or interstitials) is much higher than that of the electronic ones (electrons and holes), the high concentration of ionic carriers does not allow to build up an internal electrical field.[15–17,50] As a result, the transports of electrons and holes are driven by their chemical potential or concentration gradient governed by Fick's law of diffusion, not by migration under an electrical field. The inappropriateness of using Ohm's law is also supported by i) the deviation from the linear behavior between SSC and polarization voltage for electrochemically stable LLZO and LYC (Figure 2B) and ii) the nonzero SSC at a polarization voltage of 0 V based on the linear extrapolation of SSCs measured at lower voltages (Figure 2D).

Nevertheless, even though two-blocking-electrode cells cannot be used to determine an intrinsic electronic conductivity of SEs, the measured values can still provide important insights on the electronic transport properties of SEs. First, if the measured electronic conductivity is already negligibly small, for example, the electronic conductivity of LiPON determined by this approach is in the order of 10^{-14} to 10^{-13} S cm^{-1},[27,45] there is no need to determine the instinct values for the purpose of practical application. Second, if the polarization voltages are

sufficiently low to avoid electrolytic decomposition, the measured results can provide meaningful results for the relative magnitude of electronic conductivity, especially for the same type of SEs (sulfide, oxides, or halides) of which the defect equilibria do not change much under a specific polarization voltage. We believe the electronic conductivity determined by linear fitting of the SSC at low polarization voltages (Figure 2D) can reflect the relative magnitude for different SEs, and these values (3.0×10^{-9} S cm^{-1} for LPS, 4.5×10^{-10} S cm^{-1} for LYC, and 6.2×10^{-10} S cm^{-1} for LLZO), which are much smaller than the 10^{-7} to 10^{-9} S cm^{-1} reported in the literature (Figure 1C), can be considered as the upper limits of those SEs under these polarization voltages.

2.2. Electronic Conductivity Measurement Using Hebb–Wagner Approach

Due to the intrinsic limitation of the two-blocking-electrode cell in determining the electronic conductivity of SEs at a particular Li activity, Hebb–Wagner approach that includes a reversible electrode to define the potential should be used to measure the intrinsic electronic conductivity of SEs (see theoretical considerations of Hebb–Wagner approach in the Supporting Information).[17] It has been generally accepted by the community that Hebb–Wagner polarization method is the most viable experimental method for measuring electronic/ionic partial conductivities in mixed ionic and electronic conductors.[16,50] Nevertheless, inaccuracies also exist in the reported electronic conductivities measured using this approach due to i) instability of SEs at the anode side that can lead to interphase formation and potential variations of the reference electrode[41,51] and ii) instability of SEs at the cathode side[52] that can lead to interphase formation and ionic current to be measured. To understand the relative contribution of these sources to the inaccuracy of the measured electronic conductivity, SSCs during increasing and decreasing voltages for LLZO, LYC, and LPS SEs with different reversible electrodes (Li, Li–In, and Li–Sb) were measured, as shown in **Figure 3**. The typical current profiles during DC polarization are shown in Figure S2, Supporting Information. The utilization of high-voltage alloy anodes, Li–In with an electrode potential of ≈0.6 V versus Li/Li$^+$, and Li–Sb with an electrode potential of ≈0.9 V versus Li/Li$^+$[53] allow to study the effect of cathodic decomposition of SEs on the measurement, as the interfacial stability between SE and the reversible electrode improves as the anode potential increases.

The first observation is that for all SEs, the measured SSCs are strongly correlated with the potential of SE at the Au electrode (top *X*-axis, Figure 3) rather than the polarization voltage applied on the cell (bottom *X*-axis, Figure 3). This strongly indicates that the electronic conductivity of SEs varies with Li activity or the potential of the SE, because if the electronic conductivity is independent of Li activity, then the measured SSC would be proportional to the polarization voltage (bottom *X*-axis). This result supports that it is not appropriate to report a single value for the electronic conductivity of SEs. In addition, if we look along the horizontal direction of Figure 3, the differences between SSCs measured during increasing and decreasing voltages are larger and larger from LLZO, LYC to LPS SEs. The difference in the SSCs during increasing and decreasing voltages indicates electrolytic decompositions occurred when measuring the SSC during increasing voltages. As a result, the measured SSCs include both ionic and electronic currents and therefore cannot be used to determine the electronic conductivity of SEs. While the instability of SEs with the reversible electrode (typically Li metal) has been widely considered the main source of uncertainty for Hebb–Wagner measurements,[41] here we show that the inaccuracy of the measurement is mainly due to the anodic or oxidation decomposition of SEs. The statement is also supported by very similar values of SSCs for the cells with different reversible electrodes if we look along the vertical direction of Figure 3. Even though the decomposition of SEs with Li metal anode can lead to variations in the potential of the reference electrodes and the formation of an interphase between Li and SEs, the cathodic decomposition of SE does not influence the SSCs, probably because the formed interphase is very thin (up to hundreds of nm)[51,54] compared with the thickness of SEs (≈1 mm) and the interphase cannot contribute much to the overall electronic conductivity. On the other hand, if the anodic decomposition of SE occurs, the Li in the SE adjacent to the blocking electrode will be depleted while on the other side of the cell, Li will be inserted/alloyed/plated on the reversible electrode depending on the storage mechanism of the reversible electrode. This essentially makes the Hebb–Wagner cell a battery where Li ions pass through the SE, leading to ionic current to be measured in the SSCs. The dominant contribution of anodic decomposition SEs in the inaccuracy of the measured results is also supported by the difference of the SSCs during increasing and decreasing voltages increases with the decrease in the anodic stability of SEs from LLZO, LYC to LPS. Our results show that the anodic decomposition of SEs can lead to a much larger measurement inaccuracy than the potential variation of the reversible electrode and the interphase formation on both electrodes (Figure 3J).

2.3. Electronic Conductivities and Their Voltage Dependence of Oxide and Halide SEs

Based on the inaccuracy analysis for the Hebb–Wagner approach, it is then possible to measure the intrinsic electronic conductivity of SEs using this method if the applied potential on the blocking electrode is lower than the anodic limit of the SE and a reversible electrode that is stable with the SE is used. Based on first-principles computation, LYC is thermodynamic stable between 0.62 and 4.21 V versus Li/Li$^+$.[40] While the same computational approach also predicted that the thermodynamic electrochemical stability window of LLZO is 0.05–2.91 V, the oxidization decomposition of LLZO seems to be kinetically sluggish, as no experimental evidence has been reported for the oxidation of LLZO within typical battery operation voltages even with the addition of a significant amount of carbon.[38] The excellent anodic stability of LYC and LLZO allows us to do further data analysis using the SSCs measured from the Li–In/LLZO/Au and Li–Sb/LYC/Au cells during increasing voltages. The utilization of Li–In (0.6 V) and Li–Sb (0.9 V) with these SEs ensures that the anode is stable with SEs, as the

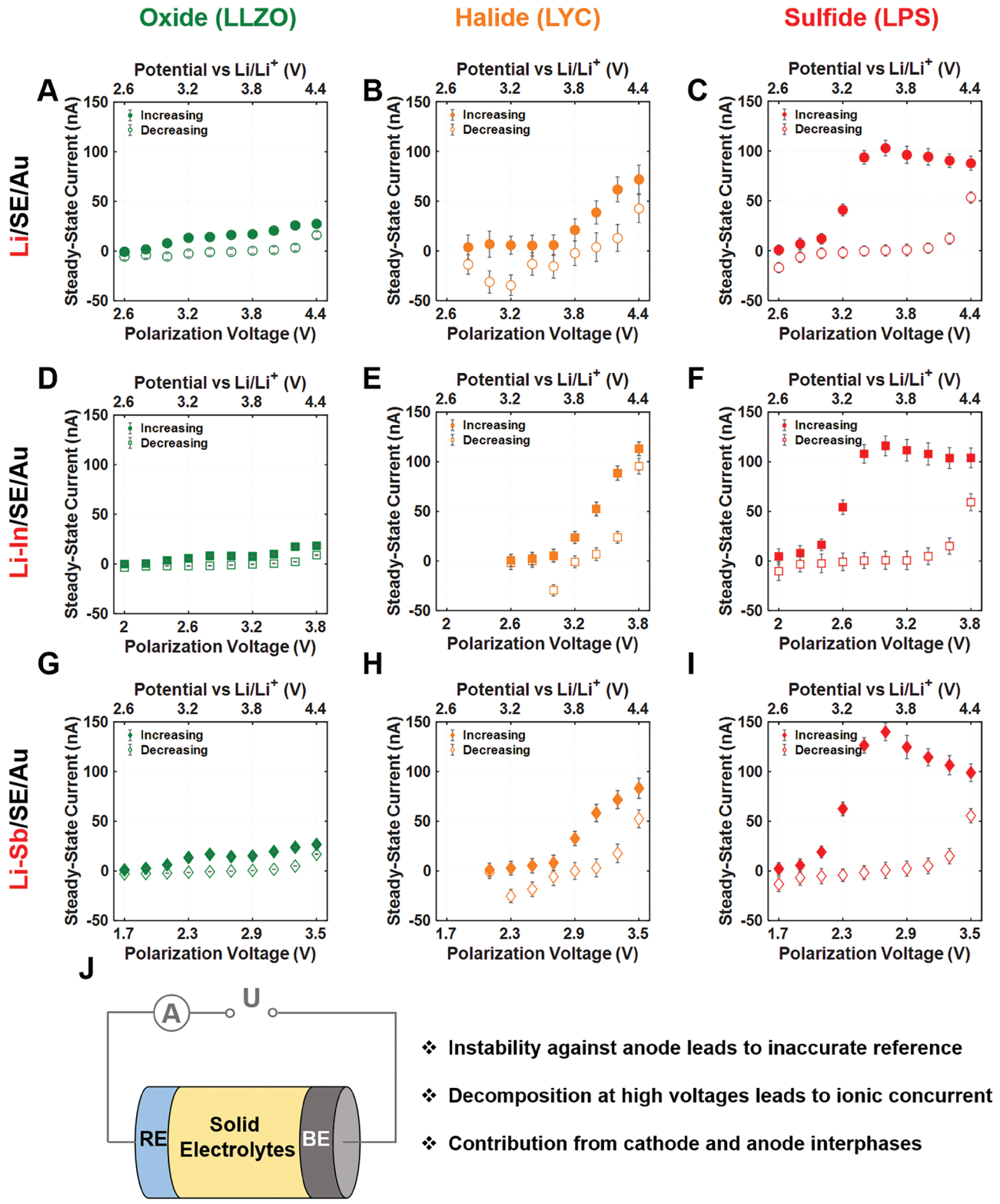

Figure 3. Steady-state currents measured from Hebb–Wagner approach. The measurements are done in cells with Au as the blocking electrode and A–C) Li (top), D–F) Li–In (middle), or G–I) Li–Sb (bottom) as the reversible electrode, and LLZO (A, D, and G, left), LYC (B, E, and F, middle), or LPS (C, F, and I, right) as the SE. The polarization voltage was gradually increased from a potential slightly higher than the OCV of the cell to a point where the potential of the Au electrode is 4.4 V versus Li/Li^+ and was then decreased back with a step size of 0.2 V. The steady-state current at each step was included in the figure. The bottom *X* axis means the polarization voltage applied on the cell and the top *X* axis means the potential of the SE at the Au electrode versus Li/Li^+. J) Sources of inaccuracy for electronic conductivity measurement using Hebb–Wagner approach.

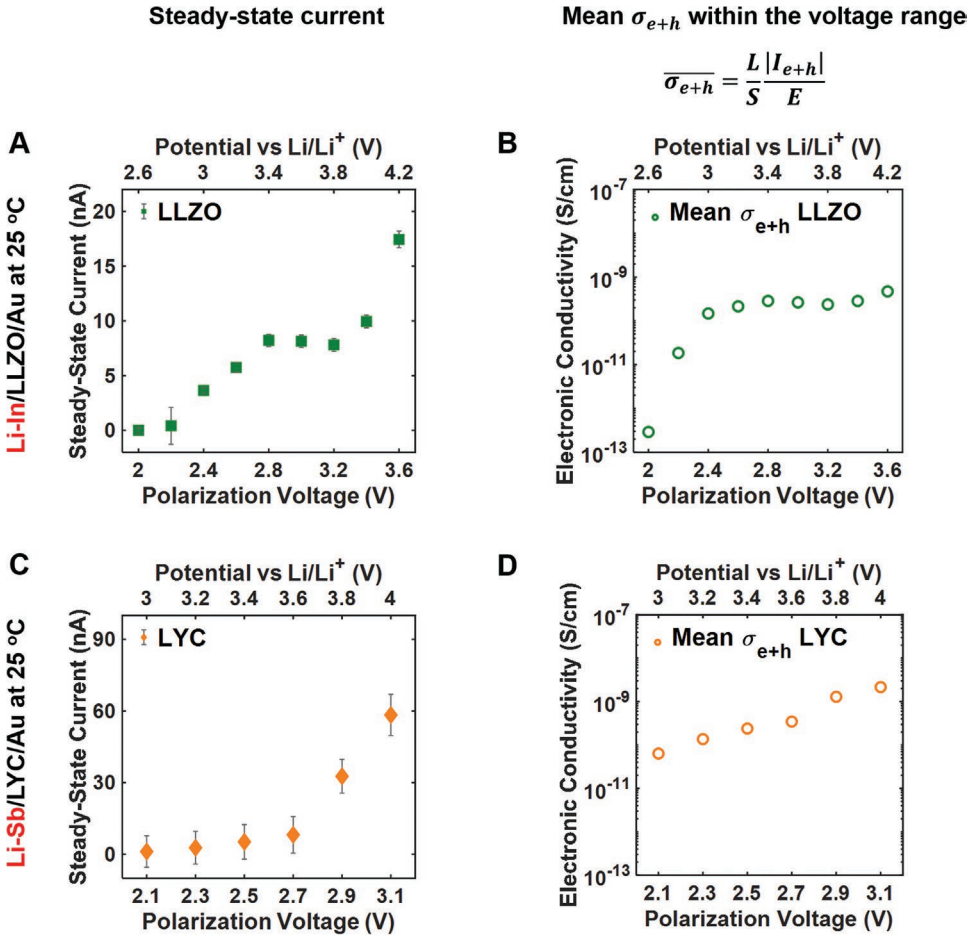

Figure 4. Steady-state currents of A) Li–In/LLZO/Au and C) Li–Sb/LYC/Au measured during increasing voltages. The mean conductivity of electron and hole, $\overline{\sigma_{e+h}}$, of LLZO (B) and D) LYC when the cells were polarized at certain voltages. $\overline{\sigma_{e+h}}$ is calculated based on Ohm's law.

thermodynamic cathodic limit for LLZO and LYC is 0.05 and 0.62 V versus Li/Li^+, respectively.[38,40] To minimize the effect of possible oxidation of SEs at high voltages, we also excluded the SSCs measured at 4.4 V for LLZO and 4.2 and 4.4 V for LYC, as shown in **Figure 4**A,C. As the SSC at each voltage can be considered as the current of the cell when the SE is polarized between the anode and the cathode, we used it to determine the mean conductivity of electron and holes $\overline{\sigma_{e+h}}$ based on Ohm's law, $\overline{\sigma_{e+h}} = \frac{L}{S} \times \frac{I}{E}$, where L is the thickness of the SE, S is the area of the SE, E is the polarization voltage, and I is the SSC. The mean electronic conductivity of LLZO (Figure 4B) increases from 4.8×10^{-12} S cm^{-1} when the SE was polarized between 0.6 (potential of Li–In electrode) and 2.1 V (potential of Au electrode) to 3.4×10^{-10} S cm^{-1} when it was polarized between 0.6 and 4.2 V. The mean electronic conductivity of LYC (Figure 4D) increases from 4.4×10^{-11} S cm^{-1} when polarized between 0.9 and 3.0 V to 1.7×10^{-9} S cm^{-1} when polarized between 0.9 and 4.0 V. These values are much lower than the reported values shown in Figure 1C. Even at 60 °C, the mean electronic conductivities of LLZO in typical battery operation voltages are still at the order of 10^{-10} S cm^{-1}. (Figure S3, Supporting Information). The increase in the mean electronic conductivity with the increased polarization voltage further confirms the voltage dependence of electronic conductivity.

Although these numbers provide important information about the averaged total electronic conductivity of SE when polarized between certain voltages, similar to the data analysis for two-blocking-electrode measurement, the utilization of Ohm's law to describe the diffusion-driven transport of electronic carriers can lead to inaccuracies in the results. The theory of Hebb–Wagner approach considers the diffusion-driven transport of electronic carriers (see Supporting Information),[15–17,50] and thus allows determination of the conductivity of electron and hole, σ_{e+h}, at a specific voltage based on equation: $\sigma = \frac{L}{S} \times \frac{dI}{dE}$. An increase in σ_{e+h} with the polarization voltage can be observed for LLZO (Figures S3 and S4A, Supporting Information) and LYC (Figure S4B, Supporting Information).

It should also be noted that the classical theory of Hebb–Wagner approach (see details in the Supporting Information) provides an accurate relation between SSC (total current of electron and hole) and polarization voltage.[16] However, the SSCs of LLZO (Figure 4A) cannot be fitted by the relation predicted by the theory. The same trend of SSC evolution was also

observed from a repeated measurement (Figure S5, Supporting Information). The exact reason for the measured behavior is currently unknown. As the Hebb–Wagner theory predicts that the SSC will increase exponentially with voltage if holes are the electronic carrier and the SSC will increase to a plateau with voltage if electrons are the carrier,[16,50] the sharp increases in the SSC at high voltages imply that holes are the electronic carrier for LLZO and LYC within the measure voltages because the concentration of holes increases with the increase of voltage (or decrease in Li activity).

2.4. A Two-Step Polarization Method to Estimate the Electronic Conductivity of Sulfide SEs

Due to the limited electrochemical stability of sulfide-based SEs (from 1.7 to 2.1 V),[38,39] there will always be electrolytic decomposition in an ion-blocking cell if the SE is polarized at a voltage beyond its stability window, and the inclusion of ionic currents in the measured SSCs precludes the possibility to do any meaningful analysis to determine its electronic conductivity. Since the decomposition of sulfide-based SEs will occur anyway in a practical SSB, it would be important and more technologically relevant if we can determine the electronic conductivity of sulfide SEs with their decomposition products. This idea leads to a modified procedure to estimate the electronic conductivity of sulfide-based SEs that decompose. As described above, the major source of the inaccuracy of Hebb–Wagner approach to determine the electronic conductivity of a SE is the anodic decomposition of the SE. However, the oxidation products of a sulfide-based SE typically contain S, P_2S_5, and other compounds depending on the composition of the SE.[39,55] Those products are highly insulating, both electronically and ionically, and the formation of these products at the cathode/SE interface can significantly suppress further decomposition of SEs. In addition, these products will not be reduced until a very low voltage of ≈2.1 V. The irreversible and self-limiting formation of oxidation products offers an opportunity to estimate the electronic conductivity of sulfide-based SE in a high-voltage cell. **Figure 5**A shows the proposed two-step polarization procedure. The sulfide-based SE, Li_6PS_5Cl, was first polarized between 0.6 V and a high voltage of 4.4 V versus Li/Li^+ to enable its complete oxidation, and then the SE was then polarized between 0.6 V and a slightly lower voltage of 4.1 V versus Li/Li^+ to determine the SSC. Since oxidation of SE occurred at 4.4 V, the SSC measured at 4.1 V would be mainly from the electronic conduction and therefore can be used to determine the electronic conductivity. Li_6PS_5Cl, instead of LPS, was used to demonstrate the proposed two-step polarization approach because the superior stability of Li_6PS_5Cl with $LiNbO_3$-coated $LiCoO_2$ cathode, as reflected from a higher initial coulombic efficiency (Figure S6, Supporting Information), enables a more accurate determination of the average electronic conductivity from the full cell aging test for validating the effectiveness of the proposed method. We used

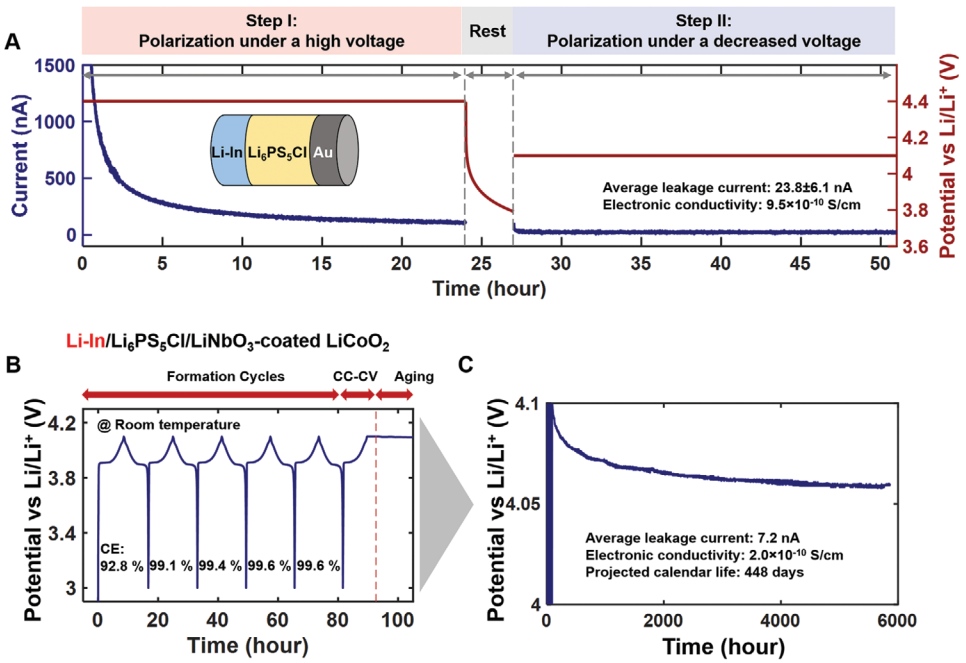

Figure 5. A) A two-step polarization method to estimate the electronic conductivity of sulfide-based SEs that decompose. Li–In/Li_6PS_5Cl/Au cell was polarized at a high cathode potential of 4.4 V versus Li/Li^+ to fully oxidize the SE prior to the measurement of the steady-state current at a slightly lower cathode potential of 4.1 V versus Li/Li^+. The steady-state current measured at the low voltage (4.1 V in this case) was then used to determine the mean electronic conductivity of SE polarized under the low voltage (4.1 V in this case). B) The average electronic conductivity of Li_6PS_5Cl SE determined from a self-discharge test of a Li–In/Li_6PS_5Cl/$LiNbO_3$ coated $LiCoO_2$ full cell at room temperature. The full cell was equilibrated at 4.1 V by a constant current–constant voltage charging before putting under rest. C) Voltage decay of the Li–In/Li_6PS_5Cl/$LiNbO_3$ coated $LiCoO_2$ full cell during calendar aging at room temperature. Li_6PS_5Cl, instead of LPS, was used to demonstrate the effectiveness of the proposed approach because the superior stability of Li_6PS_5Cl with $LiNbO_3$ coated $LiCoO_2$ cathode enables more accurate measurement of the average electronic conductivity from the full cell aging test.

4.1 V to demonstrate the proposed two-polarization method based on the following reasons. First, it is close to the charge cut-off voltage of a typical 4 V SSB and therefore the result is technologically important to predict the self-discharge rate of a charged battery. Moreover, the electronic conductivity at this voltage can also be more accurately determined from the full cell aging test. Of course, the electronic resistance measured from this approach is a result of SE and interphases, but the interphases are expected to be very thin[51,56] and may not contribute much to the overall resistance. It should be noted that the measured electronic conductivity at 4.1 V does not reflect the electrical conductivity of the SE at the same voltage, because the formed interphase can shield the electrolyte from the potential of the cathode and as a result, the electrolyte sees a potential lower than the cathode. In fact, it is not possible to measure the electronic conductivity of SE at such high voltage because the SE itself will be oxidized. Nevertheless, the measured data reflect the behavior of SEs in a real high-voltage SSB because these interphases will be formed anyway.[57]

Based on this procedure, the mean electronic conductivity of Li_6PS_5Cl SE is determined to be 9.5×10^{-10} S cm^{-1} when polarized between a 0.6 V Li–In anode and a 4.1 V Au electrode. To validate whether the measured value can reflect the behavior of the SE in an SSB, we went to the calendar aging test of a Li–In/Li_6PS_5Cl/$LiNbO_3$-coated $LiCoO_2$ full cell. The cell was cycled a few times to stabilize the interfaces and then equilibrated at 4.1 V versus Li/Li$^+$ by a constant current–constant voltage (CC–CV) charge. The cell voltage was then monitored for a few months to determine the capacity loss based on the relation between capacity and voltage measured at a low rate of 1/10 C. The average electronic conductivity was then determined by the capacity loss, assuming the capacity loss is solely caused by leakage. A similar approach was used to estimate the electronic conductivity of LiPON.[27] The average electronic conductivity for the SE polarized between a 0.6 V Li–In anode and a 4.1 V Li_xCoO_2 cathode determined from the aging test is 2.0×10^{-10} S cm^{-1}. Given the difference in the cathode for the two different approaches used here, we consider the measured electronic conductivities from the two approaches agree well with each other, validating the effectiveness of the two-step polarization method to estimate the electronic conductivity of sulfide SEs that decompose. We think the two-step polarization method can also be used to measure the electronic conductivity of other sulfide-based SEs including LPS, as the SSCs of Li_6PS_5Cl measured using the conventional approaches shows very similar behavior as LPS (Figure S7, Supporting Information). The mean electronic conductivity of LPS SE is also determined to be 2.0×10^{-10} S cm^{-1} when LPS is polarized between a 0.6 V Li–In anode and a 4.1 V Au electrode (Figure S8, Supporting Information). The same procedure can be used to determine the electronic conductivity of the SE polarized at other voltages (e.g., 3.9 and 3.7 V) to understand its voltage dependence. In this regard, one may even use the SSCs measured during decreasing voltages to estimate the electronic conductivity of sulfide-SEs polarized at different voltages. The similar value for the SSC measured from the two-step polarization measurement (23.8 nA) and the SSC determined by Hebb–Wagner measurements during decreasing voltages (34.4 nA, Figure S7, Supporting Information) supports this statement.

It should be noted that, however, voltage decay during calendar aging of a full cell can be caused by multiple mechanisms. The side reaction between oxidized $LiCoO_2$ cathode and sulfide SE may be another reason and that is also why we used a more cathode-stable SE (Li_6PS_5Cl)[58] and a $LiNbO_3$-coated $LiCoO_2$[59] to mitigate this side reaction during the aging test of the full cell. A quick voltage decay can be observed during the calendar aging of the Li–In/LPS/$LiNbO_3$-coated $LiCoO_2$ cells (Figure S9, Supporting Information). The involvement of other mechanisms for voltage decay of the full cell suggests that the average electronic conductivity determined from the aging test of a full cell (2.0×10^{-10} S cm^{-1}) can only be considered as an upper limit for the electronic conductivity of the SE. Nevertheless, given that the side reaction between a high-voltage cathode and a sulfide-SE is expected to be a diffusion-controlled process[33,34] and its reaction rate quickly decreases with time, the voltage decay at a later stage of the measurement (e.g., after 200 h) can be considered to be dominated by electronic leakage. The large portion of voltage decay occurring at the late stage of aging suggests that the average electronic conductivity of the SE should not be too much lower than 2.0×10^{-10} S cm^{-1}.

Although more studies are certainly needed to fully understand the mechanisms of capacity decay during calendar aging of a 4 V SSB based on sulfide SEs, it is unfortunate to note that the electronic conductivity of a cold-compressed sulfide SE without any intentional prior optimization does not seem to be sufficiently low to enable a long calendar life of >10 years. Based on the voltage decay, the predicted calendar life for the Li–In/Li_6PS_5Cl/$LiNbO_3$-coated $LiCoO_2$ full cell with a 1-mm-thick SE is slightly over a year (448 days) at room temperature. One can expect the calendar life will be lower if the cell was charged to a higher voltage, a thin electrolyte was used, or the cell was tested at an elevated temperature. The calendar life of the same cell tested at 60 °C is measured to be around 243 days (Figure S10, Supporting Information). While a high electronic conductivity of a SE does not preclude the utilization of the sulfide-based SE for a long-calendar-life SSB because one can always mix the SE with another insulating material such as binders or introduce a second electronic insulating layer between SE and electrodes, those approaches usually comprise the ionic conductivity of the SE. Our results here call for urgent studies on the electronic transport properties in sulfide-based SEs, including the root causes, voltage dependences, charge carriers, effects of non-stoichiometry, microstructure, surface chemistry, crystallinity, and grain/particle boundaries.[23,24,60] We would like to note that similar studies have been done to understand the electronic transport property of fuel cell electrolytes[61] and many research approaches,[50] both experimental and theoretical, can be borrowed from there.

By using a stable reversible electrode and interpreting the data within the anodic stability of SEs, we were able to show that the electronic conductivities of LLZO and LYC are at least one or two orders of magnitudes lower than the reported values within typical battery operating voltages. We were also able to show the voltage dependences of their electronic conductivities and shed light on the possible charge carrier for the electronic transport in those SEs under typical battery operating voltages. Nevertheless, the mean electronic conductivities of LLZO and

LYC seem to be still quite high when compared with the mean electronic conductivity of Li_6PS_5Cl measured by full cell aging test based on their bandgaps. The insulating interphase caused by the oxidation decomposition of sulfide SE can help explain the result. We also suspect possible oxidations of LLZO and LYC may still occur when polarizing them at high voltages due to the catalytic effects from the Au electrode. In addition, with the many assumptions made for the Hebb–Wagner approach, uncertainties also exist during the measurement of an extremely small current in a high-resistance cell. The error bars of SSCs measured vary even with the utilization of an ultra-small current module (BioLogic ULC300) and after putting the cells in a BioLogic faraday cage. We still cannot fully understand the underlying mechanisms for the evolution of SSC versus voltage for the Li–In/LLZO/Au cell at room temperature. More careful study on the uncertainty analysis of the Hebb–Wagner measurement will be needed to better use this method. Measuring the capacity decay for LLZO- or LYC- based full cells, which are currently undergoing, can provide important insights to understand the electronic conductivity of these SEs in a real SSB.

3. Conclusion

In summary, we studied the electronic conductivities of three typical SEs: LPS, LLZO, and LYC. We show that the reported electronic conductivities of SEs were overestimated from the conventional measurement. By revisiting the conventional electronic conductivity measurements including two-blocking-electrode measurement and Hebb–Wagner approach, we also discussed the sources of inaccuracy and highlighted the important role of anodic decomposition of SE in overestimating the electronic conductivity. Based on the finding, we proposed a few modifications in the electrode selection and data analysis to approach the intrinsic electronic conductivities of LLZO and LYC SEs. The voltage dependences of electronic conductivity in LLZO and LYC imply that holes, instead of electrons, are the dominant charge carriers for the electronic transport in these SEs. We also proposed a two-step polarization approach to estimate the electronic conductivity of sulfide-based SEs that decompose during measurement. Measured by the modified approaches, the electronic conductivities of all three SEs are at least one to two orders of magnitude lower than the reported values within typical battery operating voltages. This work provides a more accurate way to approach the intrinsic electronic conductivity of SEs. Nevertheless, the electronic conductivities of sulfide-based SEs still seem to be too high for a long-calendar-life SSB. Our work highlights the importance of investigating a largely ignored property of SEs and calls for a more detailed study to understand the conduction mechanisms to develop strategies to lower the electronic conductivity of SEs for future SSB development.

4. Experimental Section

Solid Electrolyte Preparation: LPS was prepared by ball milling Li_2S (Sigma-Aldrich, 99.98%) and P_4S_{10} (Sigma-Aldrich, 99%) with a stoichiometric ratio at 510 rpm for 50 h. LYC was prepared by ball milling LiCl (Alfa Aesar, 99.995%) and YCl_3 (Alfa Aesar, 99.9%) at a molar ratio of 3 to 1 at 510 rpm for 50 h. LLZO preparation followed the procedure described in the previously published literature.[31,38] Li_6PS_5Cl was prepared by solid-state synthesis method. Li_2S, P_4S_{10}, and LiCl with a stoichiometric ratio were mixed through ball milling at 110 rpm for 6 h. The mixed powders were vacuum sealed in a carbon-coated quartz tube and annealed at 550 °C for 24 h. $Li_{0.5}In$ and $Li_{11}Sb_{89}$ alloys used as the reversible electrodes were prepared by melting Li and the alloy element with appropriate molar ratios at a temperature of 50 °C higher than the melting temperature.

Cell Fabrication: The two-blocking electrode cell used in this work was prepared by sputter-coating gold (≈100 nm thick) on both sides of the solid electrolyte pellets. LPS, LYC, and Li_6PS_5Cl pellets were cold pressed a high pressure of 400 MPa for 3 min. The surface of LLZO was polished within the glovebox using 1000-grit to 5000-grit sandpapers before Au sputtering. Two stainless steel current collectors were tightened at both sides of the Au|SE|Au cell. The cells of the Hebb–Wagner measurement were prepared through a similar method but replaced one of the blocking electrodes with a reversible electrode (Li, Li–In, or Li–Sb). The cells with a blocking electrode and a reversible electrode for Hebb–Wagner measurement were stored at an elevated temperature of 60 °C overnight, prior to the measurements at room temperature, to stabilize the interface with the reversible electrode. To prepare solid-state Li–In/Li_6PS_5Cl/$LiCoO_2$ full cell, 100 mg Li_6PS_5Cl powders were first pressed at a pressure of 100 MPa. A 5 g cathode composite consisting of $LiNbO_3$ coated $LiCoO_2$ and Li_6PS_5Cl (weight ratio $LiNbO_3$ coated $LiCoO_2$:Li_6PS_5Cl = 70:30) was spread on the top of the solid electrolyte layer. The cathode and solid electrolyte were then pressed together under 350 MPa for 3 min. Li–In anode was pressed on the other side of the solid electrolyte under 300 MPa.

Electronic Conductivity Measurement: The electronic conductivity measurements using two-blocking electrode method and the Hebb–Wagner method were all performed at the electrochemical workstation (BioLogic VSP-3 Potentiostat). An ultra-low-current module (BioLogic ULC300) that can lower the base current range from 1 μA to 1 pA was also used with the potentiostat to improve the instrument's resolution to detect small currents. The electrodes for cells were properly insulated and the cells were put in a Faraday cage (BioLogic FC-45) for the electronic conductivity measurements. The polarization voltage was gradually increased from a potential slightly higher than the OCV of the cell to a point where the potential of the Au electrode was 4.4 V versus Li/Li^+ and was then decreased back with a step size of 0.2 V. The current evolution at each polarization voltage was recorded for a duration of 3 h to determine the steady-state current. For two-blocking electrode measurements, the applied DC voltage was gradually increased from 0.1 to 3 V. The steady-state currents for Hebb–Wagner measurements were measured during the increase and decrease the polarization voltages, with a step size of 0.2 V.

Supporting Information

Supporting Information is available from the Wiley Online Library or from the author.

Acknowledgements

The authors acknowledge the support from the US National Science Foundation (Award No. 2238672). F.H. also acknowledges the support from the Priti and Mukesh Chatter Career Development Chair Professorship at the Rensselaer Polytechnic Institute.

Conflict of Interest

The authors declare no conflict of interest.

Data Availability Statement

The data that support the findings of this study are available from the corresponding author upon reasonable request.

Keywords

electronic conductivity, Hebb–Wagner method, lithium-ion batteries, self-discharge, solid electrolytes

Received: November 30, 2022
Revised: February 9, 2023
Published online:

[1] J. Janek, W. G. Zeier, *Nat. Energy* **2016**, *1*, 16141.
[2] T. Inoue, K. Mukai, *ACS Appl. Mater. Interfaces* **2017**, *9*, 1507.
[3] T. Placke, R. Kloepsch, S. Dühnen, M. Winter, *J. Solid State Electrochem.* **2017**, *21*, 1939.
[4] K. Kerman, A. Luntz, V. Viswanathan, Y.-M. Chiang, Z. Chen, *J. Electrochem. Soc.* **2017**, *164*, A1731.
[5] J. Schnell, T. Günther, T. Knoche, C. Vieider, L. Köhler, A. Just, M. Keller, S. Passerini, G. Reinhart, *J. Power Sources* **2018**, *382*, 160.
[6] K. Minami, F. Mizuno, A. Hayashi, M. Tatsumisago, *Solid State Ionics* **2007**, *178*, 837.
[7] N. Kamaya, K. Homma, Y. Yamakawa, M. Hirayama, R. Kanno, M. Yonemura, T. Kamiyama, Y. Kato, S. Hama, K. Kawamoto, A. Mitsui, *Nat. Mater.* **2011**, *10*, 682.
[8] R. Kanno, M. Murayama, *J. Electrochem. Soc.* **2001**, *148*, A742.
[9] Y. Kato, S. Hori, T. Saito, K. Suzuki, M. Hirayama, A. Mitsui, M. Yonemura, H. Iba, R. Kanno, *Nat. Energy* **2016**, *1*, 16030.
[10] R. Murugan, V. Thangadurai, W. Weppner, *Angew. Chem., Int. Ed.* **2007**, *46*, 7778.
[11] T. Asano, A. Sakai, S. Ouchi, M. Sakaida, A. Miyazaki, S. Hasegawa, *Adv. Mater.* **2018**, *30*, 1803075.
[12] C. Wang, J. Liang, J. T. Kim, X. Sun, *Sci. Adv.* **2022**, *8*, eadc9516.
[13] M. H. Hebb, *J. Chem. Phys.* **1952**, *20*, 185.
[14] C. Wagner, *Proc. C. I. T. C. E., Electrochem. Semicond.* **1955**, *7*, 361.
[15] W. Weppner, J. Liu, *Z. Naturforsch. A* **1991**, *46*, 409.
[16] R. A. Huggins, *Solid State Ionics* **2001**, *143*, 3.
[17] V. Thangadurai, W. Weppner, *Chem. Mater.* **2002**, *14*, 1136.
[18] I. Riess, *Solid State Ionics* **1996**, *91*, 221.
[19] Y. Yang, Q. Wu, Y. Cui, Y. Chen, S. Shi, R.-Z. Wang, H. Yan, *ACS Appl. Mater. Interfaces* **2016**, *8*, 25229.
[20] J. Qiu, M. Wu, W. Luo, B. Xu, G. Liu, C. Ouyang, *J. Phys. Chem. C* **2021**, *125*, 23510.
[21] T. Thompson, S. Yu, L. Williams, R. D. Schmidt, R. Garcia-Mendez, J. Wolfenstine, J. L. Allen, E. Kioupakis, D. J. Siegel, J. Sakamoto, *ACS Energy Lett.* **2017**, *2*, 462.
[22] H.-K. Tian, Z. Liu, Y. Ji, L.-Q. Chen, Y. Qi, *Chem. Mater.* **2019**, *31*, 7351.
[23] P. Gorai, T. Famprikis, B. Singh, V. Stevanović, P. Canepa, *Chem. Mater.* **2021**, *33*, 7484.
[24] A. G. Squires, D. W. Davies, S. Kim, D. O. Scanlon, A. Walsh, B. J. Morgan, *Phys. Rev. Mater.* **2022**, *6*, 085401.
[25] Y. Li, P. Canepa, P. Gorai, *Phys Rev X* **2022**, *1*, 023004.
[26] B. V. Lotsch, J. Maier, *J. Electroceram.* **2017**, *38*, 128.
[27] N. J. Dudney, *Mater. Sci. Eng., B* **2005**, *116*, 245.
[28] B. Shao, S. Tan, Y. Huang, L. Zhang, J. Shi, X.-Q. Yang, E. Hu, F. Han, *Adv. Funct. Mater.* **2022**, *32*, 2206845.
[29] Y. Huang, B. Shao, F. Han, *J. Mater. Chem. A* **2022**, *10*, 12350.
[30] B. Shao, Y. Huang, F. Han, in *Solid State Batteries Volume 2: Materials and Advanced Devices* (Ed: R.-K. Gupta), American Chemical Society, Washington, DC **2022**, pp. 267–288.
[31] F. Han, A. S. Westover, J. Yue, X. Fan, F. Wang, M. Chi, D. N. Leonard, N. J. Dudney, H. Wang, C. Wang, *Nat. Energy* **2019**, *4*, 187.
[32] T. Krauskopf, F. H. Richter, W. G. Zeier, J. Janek, *Chem. Rev.* **2020**, *120*, 7745.
[33] L. Zhou, T.-T. Zuo, C. Y. Kwok, S. Y. Kim, A. Assoud, Q. Zhang, J. Janek, L. F. Nazar, *Nat. Energy* **2022**, *7*, 83.
[34] I. Kochetkov, T.-T. Zuo, R. Ruess, B. Singh, L. Zhou, K. Kaup, J. Janek, L. Nazar, *Energy Environ. Sci.* **2022**, *15*, 3933.
[35] W. Weppner, *Ionics* **2001**, *7*, 404.
[36] W. Weppner, *Ionics* **2003**, *9*, 444.
[37] T. Shimonosono, Y. Hirata, Y. Ehira, S. Sameshima, T. Horita, H. Yokokawa, *Solid State Ionics* **2004**, *174*, 27.
[38] F. Han, Y. Zhu, X. He, Y. Mo, C. Wang, *Adv. Energy Mater.* **2016**, *6*, 1501590.
[39] Y. Zhu, X. He, Y. Mo, *ACS Appl. Mater. Interfaces* **2015**, *7*, 23685.
[40] S. Wang, Q. Bai, A. M. Nolan, Y. Liu, S. Gong, Q. Sun, Y. Mo, *Angew. Chem., Int. Ed.* **2019**, *58*, 8039.
[41] S. Wenzel, D. A. Weber, T. Leichtweiss, M. R. Busche, J. Sann, J. Janek, *Solid State Ionics* **2016**, *286*, 24.
[42] Z. Wang, G. Shao, *J. Mater. Chem. A* **2017**, *5*, 21846.
[43] Y. Mo, S. P. Ong, G. Ceder, *Chem. Mater.* **2012**, *24*, 15.
[44] Y. Su, J. Falgenhauer, T. Leichtweiß, M. Geiß, C. Lupó, A. Polity, S. Zhou, J. Obel, D. Schlettwein, J. Janek, B. K. Meyer, *Phys. Status Solidi B* **2017**, *254*, 1600088.
[45] Y. Su, J. Falgenhauer, A. Polity, T. Leichtweiß, A. Kronenberger, J. Obel, S. Zhou, D. Schlettwein, J. Janek, B. K. Meyer, *Solid State Ionics* **2015**, *282*, 63.
[46] T. Ohtomo, F. Mizuno, A. Hayashi, K. Tadanaga, M. Tatsumisago, *J. Power Sources* **2005**, *146*, 715.
[47] A. Hayashi, S. Hama, H. Morimoto, M. Tatsumisago, T. Minami, *J. Am. Ceram. Soc.* **2001**, *84*, 477.
[48] A. Hayashi, H. Muramatsu, T. Ohtomo, S. Hama, M. Tatsumisago, *J. Mater. Chem. A* **2013**, *1*, 6320.
[49] L. Zhou, K.-H. Park, X. Sun, F. Lalère, T. Adermann, P. Hartmann, L. F. Nazar, *ACS Energy Lett.* **2019**, *4*, 265.
[50] W. Weppner, R. A. Huggins, *Annu. Rev. Mater. Sci.* **1978**, *8*, 269.
[51] S.-K. Otto, L. M. Riegger, T. Fuchs, S. Kayser, P. Schweitzer, S. Burkhardt, A. Henss, J. Janek, *Adv. Mater. Interfaces* **2022**, *9*, 2102387.
[52] R. Koerver, I. Aygün, T. Leichtweiß, C. Dietrich, W. Zhang, J. O. Binder, P. Hartmann, W. G. Zeier, J. Janek, *Chem. Mater.* **2017**, *29*, 5574.
[53] K. Wang, K. Jiang, B. Chung, T. Ouchi, P. J. Burke, D. A. Boysen, D. J. Bradwell, H. Kim, U. Muecke, D. R. Sadoway, *Nature* **2014**, *514*, 348.
[54] S. Wenzel, S. J. Sedlmaier, C. Dietrich, W. G. Zeier, J. Janek, *Solid State Ionics* **2018**, *318*, 102.
[55] F. Han, T. Gao, Y. Zhu, K. J. Gaskell, C. Wang, *Adv. Mater.* **2015**, *27*, 3473.
[56] F. Walther, F. Strauss, X. Wu, B. Mogwitz, J. Hertle, J. Sann, M. Rohnke, T. Brezesinski, J. Janek, *Chem. Mater.* **2021**, *33*, 2110.
[57] T.-T. Zuo, R. Rueß, R. Pan, F. Walther, M. Rohnke, S. Hori, R. Kanno, D. Schröder, J. Janek, *Nat. Commun.* **2021**, *12*, 6669.
[58] L. Zhou, N. Minafra, W. G. Zeier, L. F. Nazar, *Acc. Chem. Res.* **2021**, *54*, 2717.
[59] N. Ohta, K. Takada, I. Sakaguchi, L. Zhang, R. Ma, K. Fukuda, M. Osada, T. Sasaki, *Electrochem. Commun.* **2007**, *9*, 1486.
[60] S. Wang, W. Zhang, X. Chen, D. Das, R. Ruess, A. Gautam, F. Walther, S. Ohno, R. Koerver, Q. Zhang, W. G. Zeier, F. H. Richter, C.-W. Nan, J. Janek, *Adv. Energy Mater.* **2021**, *11*, 2100654.
[61] W. Weppner, *J. Solid State Chem.* **1977**, *20*, 305.